

# **Significant disparity in base and sugar damage in DNA by neutron and electron irradiation**

Running title: DNA base and sugar damage by neutron and electron

Authors: Dalong PANG,<sup>1,a</sup> Jeffrey S. NICO,<sup>3</sup> Lisa KARAM,<sup>3</sup> Olga TIMOFEEVA,<sup>1</sup> William F. BLAKELY,<sup>4</sup> Anatoly DRITSCHILO,<sup>1</sup> Miral DIZDAROGLU,<sup>2</sup> Pawel JARUGA<sup>2</sup>

Affiliations:

<sup>1</sup>Georgetown University Hospital, Washington, District of Columbia;

<sup>2</sup>Biomolecular Measurement Division, National Institute of Standards and Technology, Gaithersburg, Maryland;

<sup>3</sup>Radiation Physics Division, National Institute of Standards and Technology, Gaithersburg, Maryland;

<sup>4</sup>Scientific Research Department, Armed Forces Radiobiological Research Institute, Uniformed Services University of the Health Sciences, Bethesda, Maryland

<sup>a</sup>Corresponding author: Dr. D. Pang, Department of Radiation Medicine, Georgetown University Hospital, 3800 Reservoir Road, L.L. Bles, Washington, DC 20007. Email: [pangd@georgetown.edu](mailto:pangd@georgetown.edu), Office phone: (202) 444-4069 Fax: (202) 444-3786

The authors declare no conflict of interest.

Total number of pages: 22

## ABSTRACT

In this study a comparison of the effects of neutrons with electrons on irradiation of aqueous DNA solutions was investigated to characterize for potential neutron signatures on DNA damage induction. Ionizing radiations generate numerous lesions in DNA including sugar, base, base and sugar damage (i.e., 8,5'-cyclopurine-2'-deoxynucleosides), DNA-protein cross-links, single- and double-strand breaks, and clustered damage. The characteristics of damage depend on the linear energy transfer (LET) of the incident radiation. Here we investigated DNA damage using aqueous DNA solutions in 10 mmol/L phosphate buffer from 0 to 80 Gy by low-LET electrons (10 Gy/min) and high-LET neutrons (~0.16 Gy/h), the later formed by spontaneous  $^{252}\text{Cf}$  decay fissions. 8-hydroxy-2'-deoxyguanosine (8-OH-dG), (5'*R*)-8,5'-cyclo-2'-deoxyadenosine (*R*-cdA) and (5'*S*)-8,5'-cyclo-2'-deoxyadenosine (*S*-cdA) were quantified using liquid chromatography-isotope-dilution tandem mass spectrometry to demonstrate a linear dose dependence for induction of 8-OH-dG by both types of radiation, although neutrons were approximately 50 % less effective at a given dose as compared to electrons. Electron irradiation resulted in an exponential increase in *S*-cdA and *R*-cdA with dose, whereas neutrons induced substantially less damage, and the amount of damage increased only gradually with dose. Addition of 30 mmol/L 2-amino-2-(hydroxymethyl)-1,3-propanediol (TRIS), a free radical scavenger, to the DNA solution before irradiation reduced lesion induction to background levels for both types of radiation. These results provide insight into mechanisms of DNA damage by high- and low-LET radiation, leading to enhanced understanding of the potential biological effects of these radiations.

**Keywords:** electron LINAC irradiation;  $^{252}\text{Cf}$  decay fission neutrons; 8-hydroxy-2'-deoxyguanosine; (5'*R*)-8,5'-cyclo-2'-deoxyadenosine; and (5'*S*)-8,5'-cyclo-2'-deoxyadenosine; liquid chromatography-isotope-dilution tandem mass spectrometry; relative biological effectiveness

## INTRODUCTION

Ionizing radiation induces a large variety of DNA lesions, including base and sugar lesions, single strand breaks (SSBs), lesions involving base and sugar (i.e., 8,5'-cyclopurine-2'-deoxynucleosides), DNA-protein cross-links, double-strand breaks (DSBs), and clustered damaged sites [1-4]. DNA damage results by direct or indirect effect of ionizing radiation. Direct effect is a result of energy deposition directly on DNA or its closest hydration layer, whereas indirect effect is due to interaction of DNA molecules with radiation-induced free radicals generated in water such as hydroxyl radical ( $\bullet\text{OH}$ ), hydrated electron ( $e_{\text{aq}}^-$ ) and H atom ( $\text{H}\bullet$ ) [5]. Hydroxyl radicals react with the constituents of DNA near or at diffusion-controlled rates, causing damage to the heterocyclic DNA bases and to the sugar moiety by a variety of mechanisms [6]. For DNA in aqueous solution, indirect damage predominates with both low- and high-linear energy transfer (LET) radiations [6-10]; however the percentage of damage from indirect effects due to diffusible  $\bullet\text{OH}$  is reduced with high-LET radiation due to recombination reactions causing decreases in  $\bullet\text{OH}$  yields and by the presence of  $\bullet\text{OH}$  scavengers [11]. The fraction of "clustered lesions" formed at high-LET radiation in aqueous DNA solutions are relatively constant for radiation in conditions of high  $\bullet\text{OH}$  scavenging capacities, similar to that found in cell-like environments, to dilute aqueous DNA solutions [12,13].

Comparison of the effects of low- and high-LET radiations on DNA damage contributes to our knowledge of the mechanism of radiation-induced damage. The effects of heavy ions to cause single and double strand breaks are well characterized while effects on base damage and clustered lesions are less well characterized (reviewed in [14]). Neutron-induced DNA strand breaks in aqueous solution have been previously investigated [11,13,15,16]. However, no studies have been reported on neutron-induced base damage and the formation of 8,5'-cyclopurine-2'-deoxynucleosides. If not repaired by DNA repair mechanisms in living organisms, radiation-induced DNA damage may lead to disease processes such as carcinogenesis [16-19].

In the present work, we have investigated the effects of low-LET electron and high-LET neutron irradiations, the latter produced by spontaneous fission neutrons from  $^{252}\text{Cf}$  decay, on DNA base damage

using liquid chromatography-isotope dilution tandem mass spectrometry (LC-MS/MS). The resulting data provide additional insight on neutron- and electron-induction of DNA lesions, and into the physical and chemical mechanisms of neutron- and electron-induced damage to DNA.

## **MATERIALS AND METHODS**

### **Materials**

Calf thymus genomic DNA was purchased from Sigma-Aldrich (St. Louis, MO), The DNA was diluted in 10-mmol/L phosphate buffer, pH 7.4 at room temperature and aliquoted into 250- $\mu$ l Eppendorf tubes containing 60  $\mu$ g DNA each, and irradiated subsequently.

2-amino-2-(hydroxymethyl)-1,3-propanediol (TRIS) (99.9 % purity) was purchased from Sigma-Aldrich at a concentration of 30 mmol/L. Nuclease P1, snake venom phosphodiesterase, and alkaline phosphatase were purchased from United States Biological (Swampscott, MA), Sigma Chemical Co. (St. Louis, MO) and Roche Applied Science (Indianapolis, IN), respectively. Water and acetonitrile for LC-MS/MS were purchased from Sigma Chemical Co. (St. Louis, MO).

### **Electron and neutron irradiation**

Electron irradiations of DNA were performed in the Department of Radiation Medicine of Georgetown University Hospital on a medical linear accelerator (Varian Trilogy, Palo Alto, CA). The energy of the electron beam was 6 MeV. A 10 x 10 cm<sup>2</sup> electron cone was used to collimate the electron beam. The source surface distance was set at 100 cm. A 1.2-cm thick water equivalent plastic plate was placed on top of the eppendorf tubes containing the DNA samples to provide necessary dose build-up. During irradiation the DNA solution was exposed to ambient air contained in the Eppendorf tubes. Three samples were irradiated at each dose. The linear accelerator had been calibrated to deliver 1 cGy/1MU at this setting using a calibrated ion chamber traceable to the National Institute of Standards and Technology (NIST) in Gaithersburg, MD. At a dose rate of 10 Gy/min, doses of 10 , 20 40 , 60 , and 80 Gy were delivered to the samples. The uncertainty of dose was less than 2 %.

Neutron irradiations were performed at the Californium Neutron Irradiation Facility (CNIF) at NIST, using spontaneous fission neutrons from  $^{252}\text{Cf}$  decay as previously described [20,21]. To reduce the gamma component of the radiation field, a lead shield 2.1 cm in thickness was placed between the  $^{252}\text{Cf}$  source and the samples. During irradiation the DNA solution was exposed to ambient air contained in the Eppendorf tubes. The mean neutron fluence was converted to charged particle dose using the conversion factor of  $3.1 \times 10^{-11}$  Gy cm [22]. In this configuration, the gamma ray component is estimated to be 15 % based on simulation using Monte Carlo N-Particle Transport Code, Version 5 (MCNP5) [23]. Neutron irradiation times were calculated based on the known Cf-252 source activity to achieve the planned doses of 10 , 20 , 40 , 60 and 80 Gy, and they were 2.56, 5.13, 10.25,15.38 and 20.51 days, respectively. Factors affecting the accuracy of delivered doses include source position, sample position, source activity and model used for calculation. The uncertainties associated with these factors are: source position (10%), sample position (4%), source activity (3%), conversion factor (3%), modeling (3%). Together these factors contribute to a total neutron dose uncertainty of 12 %.

### **Analysis by LC-MS/MS**

We used LC-MS/MS to identify and quantify 8-hydroxy-2'-deoxyguanosine (8-OH-dG), (5'*R*)-8,5'-cyclo-2'-deoxyadenosine (*R*-cdA) and (5'*S*)-8,5'-cyclo-2'-deoxyadenosine (*S*-cdA) in DNA samples. Figure 1 shows the chemical structures of these three lesions. Stable isotope-labeled internal standards *R*-cdA- $^{15}\text{N}_5$  and *S*-cdA- $^{15}\text{N}_5$  were prepared and isolated as described [24]. 8-OH-dG- $^{15}\text{N}_5$  was purchased from Cambridge Isotope Laboratories, Inc. (Andover, MA). Aliquots of the internal standards were added to 60- $\mu\text{g}$  aliquots of DNA samples (irradiated or control). Samples were dried in a SpeedVac, subjected to enzymatic hydrolysis and analyzed by LC-MS/MS [25].

### **Statistical analysis**

All experiments involved 3 replicated samples at each dose. Arithmetic means were calculated weighting the error. Dose response yields were determined based on linear or exponential fits using least

square regression analysis. Relative biological effectiveness ratios were determined at designated product yields based on the initial linear fits to the dose response relationship. Statistical differences were determined using the Student t test at  $p < 0.05$ .

## RESULTS

Figure 2 is an illustrative example of the chromatogram of the radiation products produced in a DNA sample irradiated with 40 Gy electrons. The dose responses for the formation of 8-OH-dG, *R*-cdA, and *S*-cdA in neutron- and electron-irradiated DNA in 10 mmol/L phosphate buffer are plotted in Figure 3. Figure 4 shows the quantification of the lesions as a function of dose to electron radiations performed with and without the additional free radical scavenger TRIS at 30 mmol/L present in the solution, while the dose response with and without TRIS for neutron irradiations is given in Figure 5.

As shown in Figure 2, neutron irradiation yielded approximately 50 % of the 8-OH-dG lesions as compared to the yield following electron exposure at the same dose. The trends for both types of radiations are similar in pattern: increasing quickly in the dose range of 0 Gy to 40 Gy but less quickly from 40 Gy to 80 Gy. For *R*-cdA and *S*-cdA induction by electrons, both dose response curves exhibit exponential increases with dose over the dose range examined; however, the rate of induction of *S*-cdA is approximately half that of *R*-cdA. Neutron induction of both of these lesions is substantially less than observed with electrons, exhibiting little increases with dose. The effects of electron compared to neutron irradiation on the yields of the *R*-cdA and *S*-cdA lesions irradiated in 10 mmol/L phosphate buffer are shown in Figure 6. The ratio of *R*-cdA (light bars) and *S*-cdA (dark bars) yields caused by electrons compared to neutrons were plotted as a function of increasing dose (Fig 6A). These ratios showed a rapid increase with dose; however, the *R*-cdA ratio increased more quickly than of *S*-cdA. Furthermore, for the *R*-cdA yield, the ratio increased from 3.7 to 16.1 when the dose increased from 10 Gy to 80 Gy, nearly exponentially, while the yield of *S*-cdA showed a linear increase from 2.9 to 9.4. The effects of dose on the ability of electron and neutron to produce either the *R*-cdA vs the *S*-cdA are illustrated in Figure 6B.

Results are presented as fold changes, shown in Figure 6B as ratios in  $\log_2$  values. The relative formation of *R*-cdA to *S*-cdA is similar for the dose examined. Again electrons show a trend to produce more of *R*-cdA than *S*-cdA. These findings support a signature fingerprint for radiation quality effects when using the relative yields of these tandem lesions, *R*-cdA and *S*-cdA.

## DISCUSSION

The *R*-cdA, *S*-cdA and 8-OH-dG measured in this investigation represent the first experimental data of these DNA lesions induced by low-LET electron and high-LET neutron irradiation of genomic DNA. Single strand breaks produced by low-LET radiation are reportedly produced some 3 times that induced by fission neutrons and were attributed to the reduced yield of  $\bullet\text{OH}$  produced by the high LET radiation compared with low-LET radiation [11]. In this report, the number of the 8-OH-dG lesions per unit dose was found to increase with dose for both electron and neutron irradiation; however, at any given dose, fission neutrons from  $^{252}\text{Cf}$  decay generated half the number of these lesions, confirming a similar  $\bullet\text{OH}$  mechanism in generation of SSBs and 8-OH-dG lesions and the reduced capacity of  $\bullet\text{OH}$  induction by neutrons.

The observed induction rate differences between *R*-cdA and *S*-cdA following electron irradiation reported here are consistent with that reported by Jaruga *et al.* with photon (gamma) irradiation, which showed a ~2-fold difference in induction comparing *R*-cdA to *S*-cdA in calf thymus DNA [26]. This is not surprising considering that both electron and photon are low-LET radiation. Interestingly, while the relative ratios are consistent, the absolute numbers of lesions per Gy in  $10^6$  DNA bases are two orders of magnitude greater in Jaruga *et al.*'s earlier findings. Such difference can be explained by the conditions for sample irradiation in the presence of  $\text{N}_2\text{O}$  without oxygen, while our electron irradiations were conducted in ambient air. Oxygen is known to prevent the formation of 8,5'-cyclopurine-2'-deoxynucleosides because it rapidly reacts with the 5'-centered radical of 2'-deoxyribose of DNA inhibiting 5',8'-cyclization (reviewed in [6]). Cadet and colleagues have performed measurements of radiation-induced DNA base lesions using controlled gassing conditions [27-29]. In addition to using Co-60  $\gamma$ -rays, they measured

eight base lesions by high-LET carbon ions using LC-MS/MS, and observed a two-fold less lesion induction by carbon ions compared to photons for both thymidine glycol and 8-OH-dG in the dose range of 90 Gy to 450 Gy [30]. It should be noted that our observation of a two-fold reduction in 8-OH-dG by neutrons coincides with their findings with carbon ions although the measured base lesions are different. The LET of the carbon ions in their experiments varied from 25.2 keV/ $\mu\text{m}$  to 31.52 keV/ $\mu\text{m}$  in the irradiated cell medium. The  $^{252}\text{Cf}$  fission neutron beam in our experiments had an average energy of 2.1 MeV with a LET in the same range. Such consistency supports the LET dependence of base lesion induction regardless of the radiation applied. Interestingly, this observation for base lesions is consistent with the induction of SSB quantified with gel electrophoresis [31].

The substantially lower efficiency of neutron induction of *R*-cdA and *S*-cdA can be addressed qualitatively by the clustered nature of neutron ionization, resulting in dense formation of free radicals within each cluster, but sparsely distributed free radical clusters. The dense free radicals within each cluster have much shorter range of diffusion and higher frequency of neutralization via recombination reactions, resulting in a reduced capacity for DNA lesion induction [32,33].

While there are large differences in *R*-cdA (7-fold) and *S*-cdA (5-fold) induction by electrons and neutrons, the difference in 8-OH-dG is only two fold, suggesting differences in the mechanisms underlying the induction of 8-OH-dG and *R*-cdA or *S*-cdA (Figures 2 and 5). Previously, the total level of *R*-cdA and *S*-cdA was measured by LC-MS and GC-MS in  $\text{N}_2\text{O}$ -saturated DNA samples after exposure to  $^{60}\text{Co}$   $\gamma$ -radiation and a yield of 0.65 and 0.70 lesions per  $10^6$  DNA bases per Gy, respectively, was found [26]. 8-OH-dG was also measured by LC-MS and GC-MS and a yield of 7.77-8.06 lesions per  $10^6$  DNA bases per Gy was found [26, 34], consistent with our finding of 7.55 lesions per  $10^6$  DNA bases per Gy. *R*-cdA, *S*-cdA and 8-OH-dG are typical products of reactions of  $\bullet\text{OH}$  with DNA components. *R*-cdA and *S*-cdA are tandem lesions and formed by initial abstraction of an H atom by  $\bullet\text{OH}$  from the 5'-carbon of the sugar moiety, followed by cyclization between 5'-carbon of the sugar moiety and 8-carbon of the base moiety of the same nucleoside, and subsequent oxidation. 8-OH-dG results from  $\bullet\text{OH}$  addition to the C8-position of guanine followed by oxidation (reviewed in [35]). The rate of reaction of  $\bullet\text{OH}$  with guanine is

much faster than H-abstraction by  $\bullet\text{OH}$  from the sugar moiety of a nucleoside [35]. Furthermore, the formation of 8-OH-dG is increased by oxygen, whereas oxygen inhibits the formation of cdA. Such mechanistic differences explain the large differences in the induction by ionizing radiations of these two types of lesions (Figure 2).

The observed exponential increase with dose for *S*-cdA and *R*-cdA at higher doses may be partially explained by the large difference in dose rate for electron and neutron irradiations. At a dose rate of 10 Gy per minute, it took only 8 minutes to deliver 80 Gy for electron irradiation. On the contrary, it took slightly over 20 days to deliver 80 Gy of neutron dose. The high dose rate of electron irradiation may have resulted in a much faster depletion of oxygen contained in the air in the ependoff tubes as well as dynamic differences in the relative ion cluster density, which may have consequently resulted in an increased production of *S*-cdA and *R*-cdA.

Free radical scavengers, e.g., dimethyl sulfoxide (DMSO), glycerol, TRIS, ethanol, etc., have been widely used in DNA damage measurements in the radiation biology community to isolate and quantify the indirect damage from direct damage [36]. To examine the roles of direct vs. indirect effects of radiation on DNA lesion formation, we added free radical scavenger TRIS to the DNA solutions at a concentration of 30 mmol/L and repeated the irradiation experiments for both electron and neutrons. As shown in Figures 3 and 4, the addition of 30 mmol/L TRIS reduced the induction of all three types of lesions to background levels following either electron or neutron irradiation. To quantify the direct versus indirect effects of radiation, an order of magnitude higher dose may be required, as had been previously demonstrated by Pogozelski *et al.* in their study to isolate clustered DNA damage [13]. On the other hand, the strong effect of an  $\bullet\text{OH}$  scavenger clearly shows the formation of  $\bullet\text{OH}$  under both irradiation conditions. This is also supported by the fact that *R*-cdA, *S*-cdA and 8-OH-dG are typical products of  $\bullet\text{OH}$  reactions with DNA. 8-OH-dG may also be formed by direct effect of ionizing radiations by production of a guanine radical cation followed by reaction with water (addition of  $\bullet\text{OH}$ ) and subsequent oxidation (reviewed in [35]). However, the complete inhibition of formation of 8-OH-dG by an  $\bullet\text{OH}$  scavenger excludes the direct effect of radiation under the conditions used in this work.

In conclusion, we have demonstrated that neutrons induce a substantially lower yield of damage to DNA bases and sugars when compared to electron irradiation. The magnitude of the difference depends on the types of lesion measured: a 50 % reduction was observed for the base lesion of 8-OH-dG, while as high as 7-fold and 5-fold reductions were observed for *R*-cdA, and *S*-cdA, respectively. Taken together, these findings support a characteristic signature for the neutron radiation quality effects observed here using the yields of base and tandem DNA lesions (8-OH-dG, *R*-cdA and *S*-cdA) and complement data obtained by other investigators on neutron induced DNA DSBs and SSBs.

### **DISCLAIMERS**

Certain commercial equipment or materials are identified in this paper in order to specify adequately the experimental procedure. Such identification does not imply recommendation or endorsement by the National Institute of Standards and Technology, nor does it imply that the materials or equipment identified are necessarily the best available for the purpose. The opinions, conclusions, and recommendations expressed or implied do not necessarily reflect the views of the Department of Defense, National Institute of Standards and Technology, or any other department or agency of the U.S federal government.

## Figure legends:

FIG. 1. Chemical structures of the *R*-cdA, *S*-cdA and 8-OH-dG.

FIG. 2. Ion-current profiles of the transitions  $m/z$  250  $\rightarrow$   $m/z$  164 (*R*-cdA and *S*-cdA),  $m/z$  255  $\rightarrow$   $m/z$  169 (*R*-cdA- $^{15}\text{N}_5$  and *S*-cdA- $^{15}\text{N}_5$ ),  $m/z$  284  $\rightarrow$   $m/z$  168 (8-OH-dG) and  $m/z$  289  $\rightarrow$   $m/z$  173 (8-OH-dG- $^{15}\text{N}_5$ ) recorded during the LC-MS/MS analysis of a DNA sample irradiated with electrons at dose 40 Gy.

FIG. 3. Dose responses of 8-OH-dG (panel A), *R*-cdA (panel B) and *S*-cdA (panel C) induced by irradiation with electrons at 10 Gy/min (dark columns) and neutrons at  $\sim$ 0.16 Gy/h (light columns). Each data point represents the mean of three independent measurements. The uncertainties are standard deviations.

FIG. 4. Comparison of electron-radiation induced 8-OH-dG (panel A), *R*-cdA (panel B) and *S*-cdA (panel C) with (light columns) and without (“dark columns”) the free radical scavenger TRIS. The missing data points at 60 Gy for electron irradiation with TRIS were due to an accidental damage of the samples. Each data point represents the mean of three independent measurements. The uncertainties are standard deviations.

FIG. 5. Comparison of neutron-radiation induced 8-OH-dG (panel A), *R*-cdA (panel B) and *S*-cdA (panel C) with (light columns) and without (dark columns) the free radical scavenger TRIS. The missing data points at 60 Gy for neutron irradiation with TRIS were due to an accidental damage of the samples. Each data point represents the mean of three independent measurements. The uncertainties are standard deviations.

FIG.6. Neutron vs. electron effect signatures using relative product yields of *R*-cdA and *S*-cdA. A) Ratios of the yield of *R*-cdA and *S*-cdA lesions induced by electron relative to neutron irradiation. The light columns represent data points for *R*-cdA, and the dark columns represent data points for *S*-cdA. B) Ratios of the yield of *R*-cdA relative to *S*-cdA for electrons and neutrons. Dark circles represent electrons and light boxes represent neutrons. Each data point represents the mean of three independent measurements. The uncertainties are standard deviations.

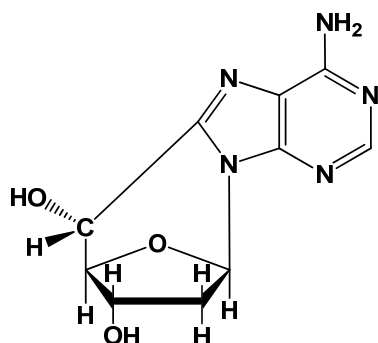
## REFERENCES

1. von Sonntag C. The chemistry of free-radical-mediated DNA damage. *Basic Life Sci.* 1991;**58**:287-317.
2. Dizdaroglu M, von Sonntag C, Schulte-Frohlinde D. Dizdaroglu M, von Sonntag C, Schulte-Frohlinde D. Letter: Strand breaks and sugar release by gamma-irradiation of DNA in aqueous solution. *J Am Chem Soc.* 1975;**97**:2277-8.
3. Chatterjee A, Holley WR. Early chemical events and initial DNA damage. *Basic Life Sci.* 1991;**58**:257-79.
4. Frankenberg-Schwager M. Induction, repair and biological relevance of radiation-induced DNA lesions in eukaryotic cells. *Radiat Environ Biophys.* 1990;**29**:273-92.
5. Goodhead DT. Initial events in the cellular effects of ionizing radiations: clustered damage in DNA. *Int J Radiat Biol.* 1994;**65**:7-17.
6. von Sonntag C. Free radical induced DNA damage and its repair: a chemical perspective. Springer, 2006.
7. Douki T, Ravanat JL, Pouget JP, Testard I, Cadet J. Minor contribution of direct ionization to DNA base damage induced by heavy ions. *Int J Radiat Biol.* 2006;**82**:119-27.
8. Kuimova MK, Cowan AJ, Matousek P, Parker AW, Sun XZ, Towrie M, et al. Monitoring the direct and indirect damage of DNA bases and polynucleotides by using time-resolved infrared spectroscopy. *Proc Natl Acad Sci U S A.* 2006;**103**:2150-3.
9. Cadet J, Bellon S, Douki T, Frelon S, Gasparutto D, Muller E, et al. Radiation-induced DNA damage: formation, measurement, and biochemical features. *J Environ Pathol Toxicol Oncol.* 2004;**23**:33-43.
10. Jones GD, Boswell TV, Lee J, Milligan JR, Ward JF, Weinfeld M. A comparison of DNA damages produced under conditions of direct and indirect action of radiation. *Int J Radiat Biol.* 1994;**66**:441-5.
11. Stankus AA, Xapsos MA, Kolanko CJ, Gerstenberg HM, Blakely WF. Energy deposition events produced by fission neutrons in aqueous solutions of plasmid DNA. *Int J Radiat Biol.* 1995;**68**:1-9.

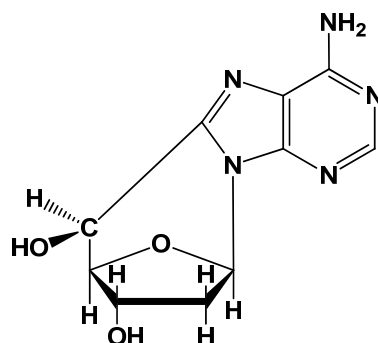
12. Xapsos MA, Pogozielski WK. Modeling the yield of double-strand breaks due to formation of multiply damaged sites in irradiated plasmid DNA. *Radiat Res.* 1996;**146**:668-72.
13. Pogozielski WK, Xapsos MA, Blakely WF. Quantitative assessment of the contribution of clustered damage to DNA double-strand breaks induced by <sup>60</sup>Co gamma rays and fission neutrons. *Radiat Res.* 1999;**151**:442-8.
14. Cadet J, Girault I, Gromova M, Molko D, Odin F, Polverelli M. Effects of heavy ions on nucleic acids: measurement of the damage. *Radiat Environ Biophys.* 1995;**34**:55-7.
15. Spothem-Maurizot M, Charlier M, Sabattier R. DNA radiolysis by fast neutrons. *Int J Radiat Biol.* 1990;**57**:301-13.
16. Spothem-Maurizot M, Franchet J, Sabattier R, Charlier M. DNA radiolysis by fast neutrons. II. Oxygen, thiols and ionic strength effects. *Int J Radiat Biol.* 1991;**59**:1313-24.
17. Wallace SS. Biological consequences of free radical-damaged DNA bases. *Free Radic BiolMed* 2002;**33**:1-14.
18. Evans MD, Dizdaroglu M, Cooke MS. Oxidative DNA damage and disease: induction, repair and significance. *Mutat Res* 2004;**567**:1-61.
19. Friedberg EC, Walker GC, Siede W, Wood RD, Schultz RA, Ellenberger T. *DNA Repair and Mutagenesis.* Washington, D.C.: ASM Press; 2006.
20. Grundl JA, Spiegel V, Eisenhauer CM *et al.*, A californium-<sup>252</sup> fission spectrum irradiation facility for neutron reaction rate measurements. *Nucl. Technol.* 1977;**32**: 315-19.
21. Lamaze GP and Grundl JA, Activation foil irradiation with californium fission sources, *NBS Spec. Publ.* 1988; 250-13: 1-17.
22. International Organization for Standardization (ISO), Neutron reference radiations for calibrating neutron-measuring devices used for radiation protection purposes and for determining their response as a function of neutron energy, Annex B (normative). 1989; 8529: 17.

23. X-5 Monte Carlo Team, MCNP – A General Monte Carlo N-Particle Transport Code, Version 5, LANL Report LA-UR-03-1987, Los Alamos (2008).
24. Birincioglu M, Jaruga P, Chowdhury G, Rodriguez H, Dizdaroglu M, Gates KS. DNA base damage by the antitumor agent 3-amino-1,2,4-benzotriazine 1,4-dioxide (tirapazamine). *Amer. Chem. Soc.* 2003;**125**:11607-11615.
25. Jaruga P, Xiao Y, Nelson BC, Dizdaroglu. Measurement of (5'R)- and (5'S)-8,5'-cyclo-2'-deoxyadenosine in DNA *in vivo* by liquid chromatography/isotope-dilution mass spectrometry. *Biochem. Biophysic. Res. Com.* 2009;**386**:656-660.
26. Dizdaroglu M, Jaruga P, Rodriguez H. Identification and quantification of 8,5'-cyclo-2'-deoxyadenosine in DNA by liquid chromatography/ mass spectrometry. *Free Radic Biol Med.* 2001;**30**:774-84.
27. Cadet J, Douki T, Ravanat JL. Measurement of oxidatively generated base damage in cellular DNA. *Mutat Res.* 2011;**711**:3-12.
28. Belmadoui N, Boussicault F, Guerra M, Ravanat JL, Chatgililoglu C, Cadet J. Radiation-induced formation of purine 5',8-cyclonucleosides in isolated and cellular DNA: high stereospecificity and modulating effect of oxygen. *Org Biomol Chem.* 2010;**8**:3211-9.
29. Regulus P, Spessotto S, Gateau M, Cadet J, Favier A, Ravanat JL. Detection of new radiation-induced DNA lesions by liquid chromatography coupled to tandem mass spectrometry. *Rapid Commun Mass Spectrom.* 2004;**18**:2223-8.
30. Pouget JP, Frelon S, Ravanat JL, Testard I, Odin F, Cadet J. Formation of modified DNA bases in cells exposed either to gamma radiation or to high-LET particles. *Radiat Res.* 2002;**157**:589-95.
31. Purkayastha S, Milligan JR, Bernhard WA. On the chemical yield of base lesions, strand breaks, and clustered damage generated in plasmid DNA by the direct effect of X rays. *Radiat Res.* 2007;**168**:357-66.

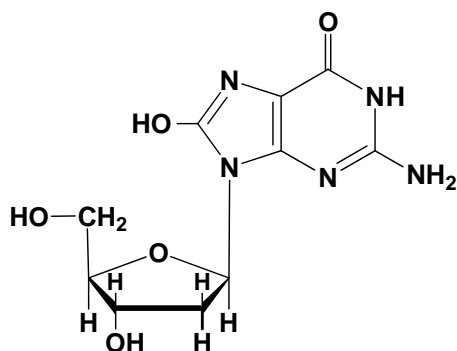
32. Leloup C, Garty G, Assaf G, Cristovão A, Breskin A, Chechik R, et al. Evaluation of lesion clustering in irradiated plasmid DNA. *Int J Radiat Biol.* 2005;**81**:41-54.
33. Milligan JR, Aguilera JA, Wu CC, Paglinawan RA, Nguyen TT, Wu D, et al. Effect of hydroxyl radical scavenging capacity on clustering of DNA damage. *Radiat Res.* 1997;**148**:325-9.
34. Jaruga P, Birincioglu M, Rodriguez H, Dizdaroglu M. Mass spectrometric assays for the tandem lesion 8,5'-cyclo-2'-deoxyguanosine in mammalian DNA. *Biochemistry.* 2002;**41**:3703-11
35. Dizdaroglu M, Jaruga P. Mechanisms of free radical-induced damage to DNA. *Free Radic Res.* 2012;**46**:382-419.
36. Milligan JR, Aguilera JA, Wu CC, Paglinawan RA, Nguyen TT, Wu D, Ward JF. Effect of hydroxyl radical scavenging capacity on clustering of DNA damage. *Radiat Res.* 1997;**148**:325-9.



**(5'R)-8,5'-cyclo-2'-deoxyadenosine**



**(5'S)-8,5'-cyclo-2'-deoxyadenosine**



**8-hydroxy-2'-deoxyguanosine**

**Fig. 1**

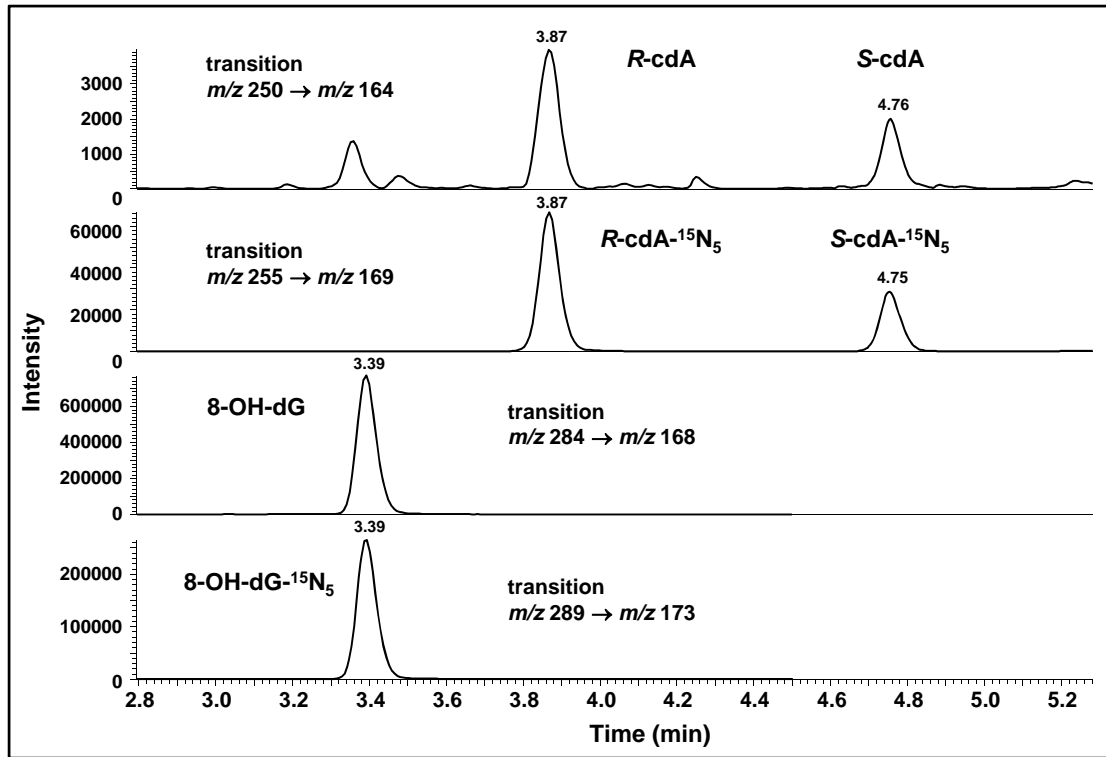


Fig. 2

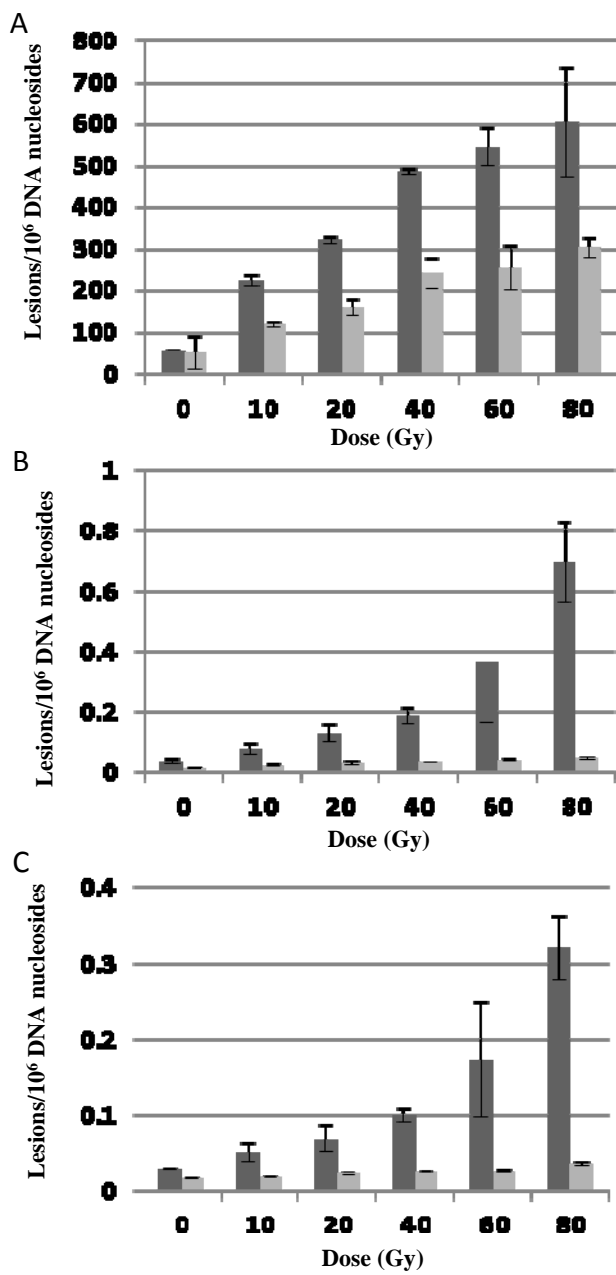


Fig. 3

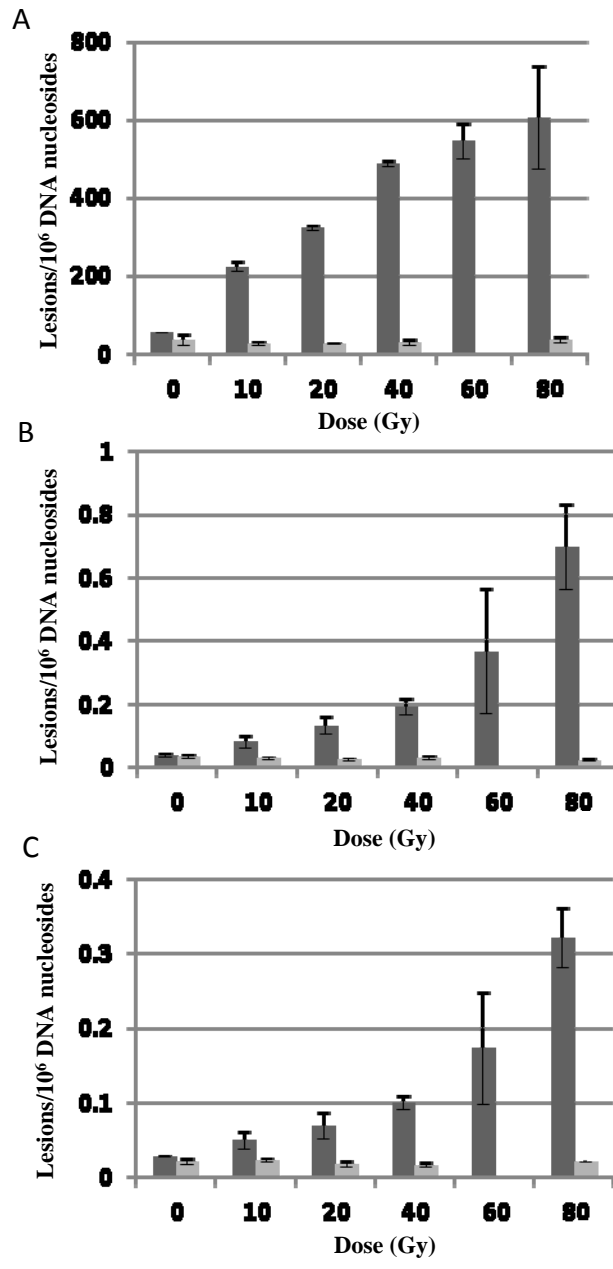


Fig. 4

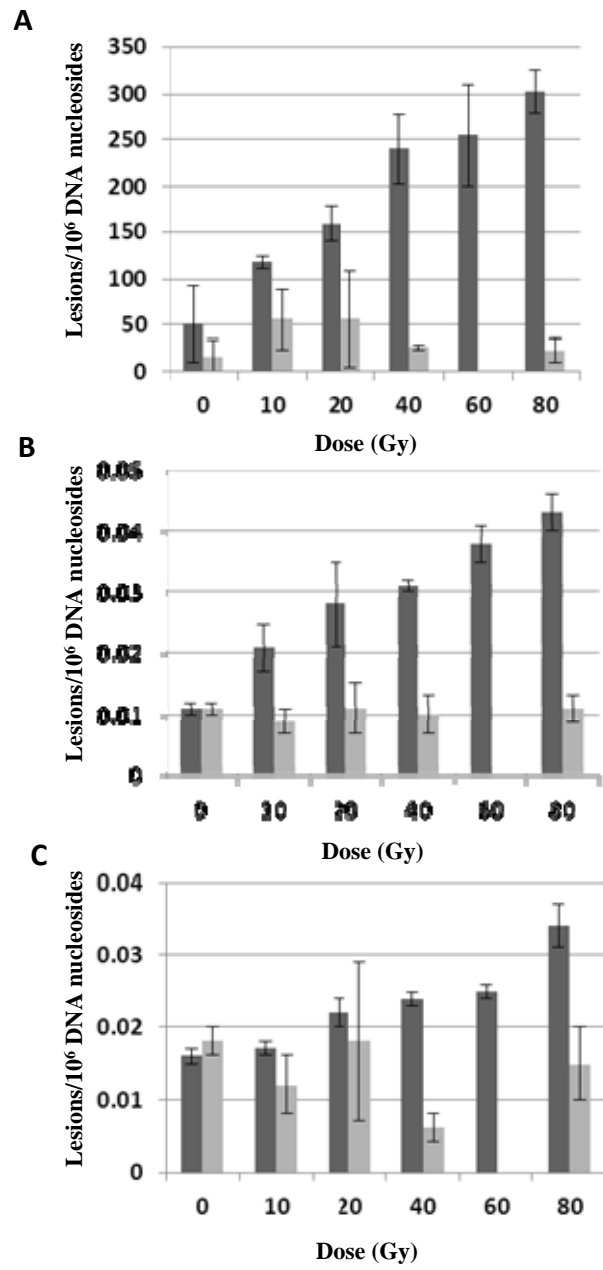
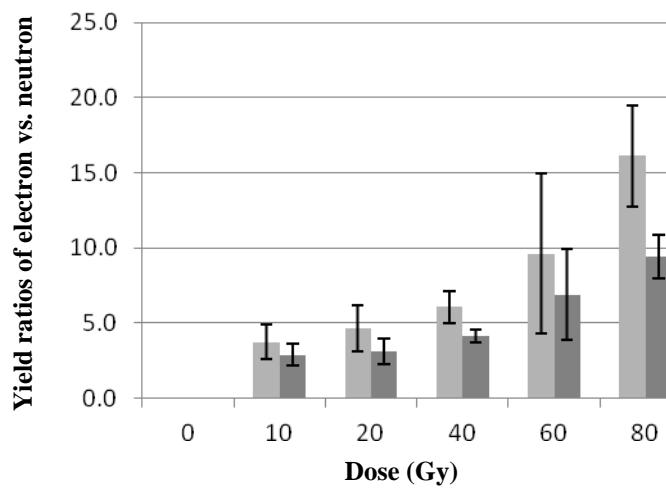


Fig. 5

A



B

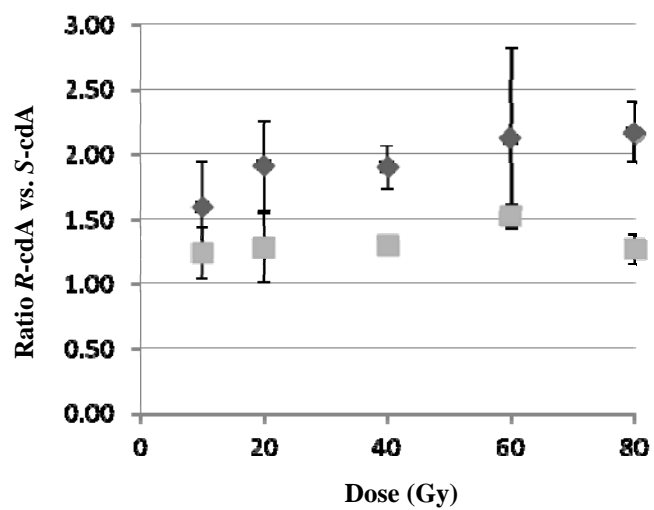


Fig. 6